Long period fiber grating formed by periodically structured microholes in all-solid photonic bandgap fiber

Minwei Yang[1], D. N. Wang[1*], Ying Wang[1, 2], Changrui Liao[1]

[1]*Department of Electrical Engineering, The Hong Kong Polytechnic University, Hung Hom, Kowloon, Hong Kong, P.R. China*

[2]*Wuhan National Laboratory for Optoelectronics, Huazhong University of Science and Technology, Wuhan 430074, P.R. China*

**eednwang@polyu.edu.hk*

Abstract: A new type long period fiber grating is fabricated in all-solid photonic bandgap fiber by periodically drilling microholes using femtosecond laser pulse irradiation. Such a structure introduces a strong refractive index modulation in the waveguide structure and hence exhibits a compact grating dimension. Both the simulation and the experimental results confirm the existence of the light coupling from core mode to the LP_{11} cladding mode. The refractive index sensing capability of the device has been investigated and the resonant wavelength shift corresponding to the refractive index change from 1.30 to 1.35 is 23.7nm. The average refractive index sensitivity obtained is 537nm/RIU (refractive index unit).

OCIS codes: (050.2770) Gratings; (060.2370) Fiber optics sensors; (060.7140) Ultrafast process in fibers.

References and links

1. A. M. Vengsarkar, P. J. Lemaire, J. B. Judkins, V. Bhatia, T. Erdogan, and J. E. Sipe, "Long-period fiber gratings as band rejection filters," J. Lightwave Technol. **14**(1), 58–65 (1996).
2. P. Steinvurzel, E. D. Moore, E. C. Mägi, B. T. Kuhlmey, and B. J. Eggleton, "Long period grating resonances in photonic bandgap fiber," Opt. Express **14**(7), 3007–3014 (2006).
3. Y. Wang, W. Jin, J. Ju, H. Xuan, H. L. Ho, L. Xiao, and D. N. Wang, "Long period gratings in air-core photonic bandgap fibers," Opt. Express **16**(4), 2784–2790 (2008).
4. L. Jin, Z. Wang, Y. Liu, G. Kai, and X. Dong, "Ultraviolet-inscribed long period gratings in all-solid photonic bandgap fibers," Opt. Express **16**(25), 21119–21131 (2008).
5. F. Luan, A. K. George, T. D. Hedley, G. J. Pearce, D. M. Bird, J. C. Knight, and P. St. J. Russell, "All-solid photonic bandgap fiber," Opt. Lett. **29**(20), 2369–2371 (2004).
6. A. Bétourné, G. Bouwmans, Y. Quiquempois, M. Perrin, and M. Douay, "Improvements of solid-core photonic bandgap fibers by means of interstitial air holes," Opt. Lett. **32**(12), 1719–1721 (2007).
7. Y. Li, D. N. Wang, and L. Jin, "Single-mode grating reflection in all-solid photonic bandgap fibers inscribed by use of femtosecond laser pulse irradiation through a phase mask," Opt. Lett. **34**(8), 1264–1266 (2009).
8. C. Florea, and K. A. Winick, "Fabrication and characterization of photonic devices directly written in glass using femtosecond laser pulses," J. Lightwave Technol. **21**(1), 246–253 (2003).
9. M. D. Perry, B. C. Stuart, P. S. Banks, M. D. Feit, V. Yanovsky, and A. M. Rubenchik, "Ultrashort-pulse laser machining of dielectric materials," J. Appl. Phys. **85**(9), 6803–6810 (1999).
10. A. Marcinkevičius, S. Juodkazis, M. Watanabe, M. Miwa, S. Matsuo, H. Misawa, and J. Nishii, "Femtosecond laser-assisted three-dimensional microfabrication in silica," Opt. Lett. **26**(5), 277–279 (2001).
11. E. N. Glezer, and E. Mazur, "Ultrafast-laser driven micro-explosions in transparent materials," Appl. Phys. Lett. **71**(7), 882–884 (1997).
12. Y. Li, K. Itoh, W. Watanabe, K. Yamada, D. Kuroda, J. Nishii, and Y. Jiang, "Three-dimensional hole drilling of silica glass from the rear surface with femtosecond laser pulses," Opt. Lett. **26**(23), 1912–1914 (2001).
13. A. van Brakel, C. Grivas, M. N. Petrovich, and D. J. Richardson, "Micro-channels machined in microstructured optical fibers by femtosecond laser," Opt. Express **15**(14), 8731–8736 (2007).
14. Y. Kondo, K. Nouchi, T. Mitsuyu, M. Watanabe, P. G. Kazansky, and K. Hirao, "Fabrication of long-period fiber gratings by focused irradiation of infrared femtosecond laser pulses," Opt. Lett. **24**(10), 646–648 (1999).
15. A. I. Kalachev, D. N. Nikogosyan, and G. Brambilla, "Long-period fiber grating fabrication by high-intensity femtosecond pulses at 211 nm," J. Lightwave Technol. **23**(8), 2568–2578 (2005).

#120871 - $15.00 USD Received 2 Dec 2009; revised 11 Jan 2010; accepted 11 Jan 2010; published 19 Jan 2010

16. T. Allsop, M. Dubov, A. Martinez, F. Floreani, I. Khrushchev, D. J. Webb, and I. Bennion, "Bending characteristics of fiber long-period gratings with cladding index modified by femtosecond laser," J. Lightwave Technol. **24**(8), 3147 (2006).
17. I. M. White, and X. Fan, "On the performance quantification of resonant refractive index sensors," Opt. Express **16**(2), 1020–1028 (2008).
18. J. H. Chong, P. Shum, H. Haryono, A. Yohana, M. K. Rao, and C. Lu, "Measurements of refractive index sensitivity using long-period grating refractometer," Opt. Commun. **229**(1-6), 65–69 (2004).
19. X. Shu, L. Zhang, and I. Bennion, "Sensitivity Characteristics of Long-Period Fiber Gratings," J. Lightwave Technol. **20**(2), 255–266 (2002).
20. L. Rindorf, and O. Bang, "Highly sensitive refractometer with a photonic-crystal-fiber long-period grating," Opt. Lett. **33**(6), 563–565 (2008).

1. Introduction

Long period fiber grating (LPFG) possesses a periodical refractive index (RI) modulation along the fiber length, which enables the light energy coupling from the fundamental mode to the cladding mode and hence creating resonant dips in its transmission spectrum [1]. LPFG can be inscribed in various types of optical fibers such as photonic bandgap fiber (PBGF) [2–4], which confines light through the bandgap mechanism instead of total internal reflection, exhibits different dispersion and nonlinear properties when compared with normal communication single mode fiber (SMF) and as a result, has received increased research attentions nowadays [5, 6]. PBGF is divided into two types, air core and all-solid PBGF. Compared with the air core PBGF, all solid PBGF has the advantage of easy fabrication and small splicing loss between the all-solid PBGF and conventional SMF as no air hole collapse occurs [7].

One of the attractive means to fabricate LPFG is by use of femtosecond laser which allows the inscription of LPFG without the requirement of photosensitivity [8]. The femtosecond laser exhibits an extremely high light intensity over an ultrashort pulse duration which makes it a powerful tool for high precision ablation [9]. The materials can be removed in a fast and clean way, with negligible heat affected zones, thus avoiding any significant damage to the underlying substrate [10]. Such clean and high precision femtosecond laser pulses ablation is well suited for micromachining applications in optical waveguides and optical fibers.

Recently, microhole and micro-channel drilling in silica glass by the use of femtosecond laser pulses has been achieved in a highly reproducible way [11, 12], and the devices created can be used as gas or fluid sensors [13]. It is interesting to note that when a series of microholes are arranged to be periodically positioned along the fiber length, a new type of LPFGs could be effectively created.

In this paper, LPFG based on periodically structured microholes has been fabricated in all-solid PBGF by use of femtosecond laser micromachining. On contrary to the conventional LPFG fabricated by femtosecond laser [14–16], the air-hole structured LPFG introduces a strong RI modulation in the fiber core and cladding, which effectively couples light from the fundamental core mode to the cladding mode in a relatively efficient way by supporting a small grating dimension. The modes involved in the coupling are also examined and the experimental results obtained are compared with those of the numerical simulations. RI sensing by use of the LPFG developed has also been carried out.

2. Experiment setup and spectrum

In the experiment, femtosecond laser pulses (with central wavelength of 800nm, pulse duration time of 120fs and repetition rate of 1 kHz) are focused onto the PBGF cladding surface through a 20× objective lens (with an NA value of 0.5, energy coupling efficiency of 0.8 and a working distance of 2.1mm). The pulse energy is set as 6.3μJ and kept constant during the fabrication. The non-photosensitive PBGF used has 5 layers of high RI rods with a period of 9.6μm. A buffering loop (with the diameter of 7.3μm) lies around each rod. The refractive indices (at 1550nm) of the high RI rod, the buffering loop and the cladding are 1.4807, 1.4356, and 1.444, respectively. During the experiment, PBGF is mounted on a three dimensional translation stage controlled by a computer, with a tuning resolution of 40nm. The pulse energy and exposure time (~40s) are chosen to fabricate microholes with depth close to

#120871 - $15.00 USD Received 2 Dec 2009; revised 11 Jan 2010; accepted 11 Jan 2010; published 19 Jan 2010

the PBGF radius. After laser pulse irradiation, part of the fiber material is removed and a cone shape microhole is created. The scale of the microhole is about 62μm in depth with a cone angle of 5 degree (this corresponds to 11μm in width at the cladding surface). By drilling microholes periodically, a structural modulated LPFG device is fabricated. Figure 1 shows the cross section of the original PBGF, the PBGF with microhole and the side view of the microhole (the two horizontal lines in Figs. 1(a) and 1(b) are the synchronized noise of CCD).

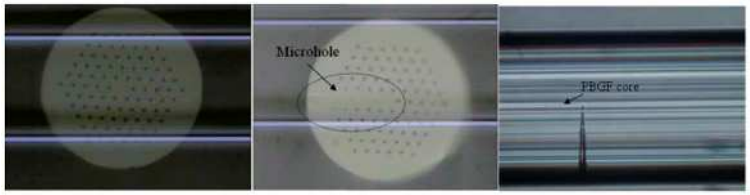

Fig. 1. Cross section view of the PBGF used in the experiment (a) without microhole (b) with microhole (c) side view of microhole.

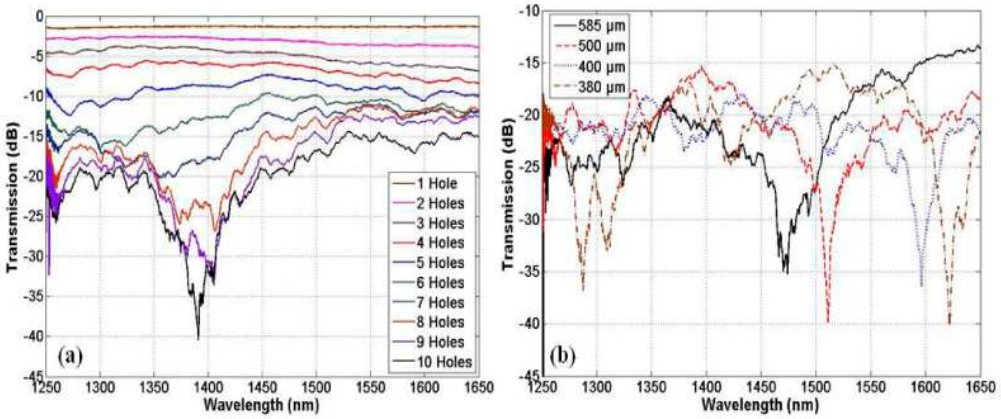

Fig. 2. Transmission spectra of the LPFG (a) Evolution of the transmission spectrum of the LPFG with the number of the microhole (b) Transmission spectrum of LPFG samples with different periods. The cladding mode is considered to be an LP_{11} like mode.

The transmission spectrum of the LPFG is measured by an OSA (AQ3619, Yokogawa) with a resolution set as 0.5nm. The evolution of the transmission spectrum of one LPFG sample with a period of 610μm is shown in Fig. 2(a). The resonant wavelength of the device is located at 1390.9nm. The insertion loss is 14.40dB and the resonant depth is 25.96dB (which is defined as the difference between the transmission loss at the resonant wavelength and the insertion loss). The high insertion loss may be due to the following reasons: 1) the fabrication will remove part of the fiber core; 2) the surface roughness of the microhole may result in light scattering; and 3) the small difference in the focus position and the hole size for each microhole, which affects the uniformity of the grating structure and leads to the increase of the light scattering. Thus, in order to improve the grating behavior, a more precise focus position should be achieved. Besides, the pulse energy and the irradiation time should also be carefully adjusted as smaller pulse energy together with longer irradiation time result in a smoother inner hole surface. Figure 2(b) demonstrates the transmission spectra for the LPFGs with different periods under the same laser exposure condition, as those shown in Fig. 2(a). The grating periods are 585, 500, 400 and 380μm, with the corresponding resonant wavelengths of 1474.2, 1510.9, 1596.2 and 1621.4nm, respectively. These LPFGs have the period number of 10, 11, 8 and 11, respectively. The spectra shown in Fig. 2 are not so clean, which is due to the noise of the broadband light source used in the experiment. The resonant wavelength of each sample is determined by measuring the dip value of the transmission

#120871 - $15.00 USD Received 2 Dec 2009; revised 11 Jan 2010; accepted 11 Jan 2010; published 19 Jan 2010

spectrum. For example, in Fig. 2(b), the spectra are smooth at their dips and the resonant wavelengths can be determined unambiguously except for that with the period of 585μm.

The total length of the LPFGs fabricated by femtosecond laser micromachining is much smaller than that written in normal SMF (with a dimension of several centimeters). According to the grating theory, the transmission T can be determined by the coupling coefficient κ and the grating length L from the relationship $T=cos^2(\kappa L)$ [4], the microhole-structured LPFG possesses a much stronger RI modulation than LPFG fabricated in normal SMF.

The polarization dependent property of the device proposed is studied in another sample with the period of 400μm. A fiber polarizer is used to change the broadband light into a certain state of polarization (SOP) and a polarization controller is used to change the SOP. The maximum resonant wavelength change is 1nm (from 1598 to 1597nm) and the maximum polarization dependent loss (PDL) obtained is 7.6dB, as shown in Fig. 3. The high PDL may be induced by the one side structure modulation, which results in a strong asymmetry in fiber waveguide and affects the birefringence of both the core mode and the cladding modes.

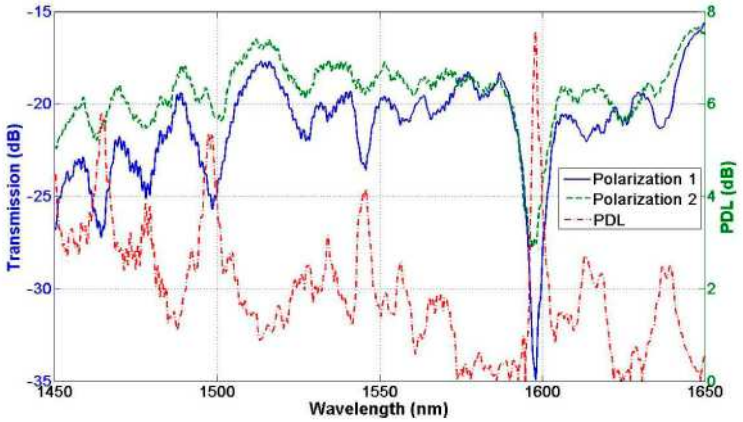

Fig. 3. Polarization dependent property of a sample with the period of 400μm.

3. Mode field analysis

Jin *et al* [4] has demonstrated that for the LPFG fabricated in all-solid PBGF, the mode coupling may occur between the fundamental core mode and either cladding modes or guided supermodes. In order to identify the modes involved, the sample shown in Fig. 2(a) is cut off at the grating end and its near mode field is measured by an infrared CCD (Electrophysics, 7290A) and a tunable laser (Agilent 8164B). Figure 4 shows the fundamental mode and the cladding mode when the external RI is 1.32 (this changes the resonant wavelength of the sample to 1500.3nm so as to fit in the minimum wavelength of the tunable laser at 1494nm).

Figure 4(a) shows the fundamental mode of the sample, where most of the light energy is confined in the fiber core except one high RI rod (this may due to the surface roughness of the cross section induced by cutting). Figure 4(b) shows the mode profile at the resonant wavelength and when compared with that in Fig. 4(a), it is clear that the fundamental mode has split into three parts. This mode field profile is considered to be from the LP_{11} mode: the upper half (along the laser irradiating direction) of the LP_{11} mode is split into two parts by the microhole structure; while the lower half of the LP_{11} profile remains without obvious deformation. This phenomenon agrees with the simulation result obtained by use of finite element method (FEM), as shown in Fig. 4(c) ~Fig. 4(f), which displays the mode field near the fiber core. In the simulation results, the black arrows represent both the direction and the magnitude of the modes electric field. The simulation demonstrates that both the core mode and the cladding mode have two fold symmetry: one with electric field direction parallel to the microhole and the other perpendicular to the microhole.

#120871 - $15.00 USD Received 2 Dec 2009; revised 11 Jan 2010; accepted 11 Jan 2010; published 19 Jan 2010

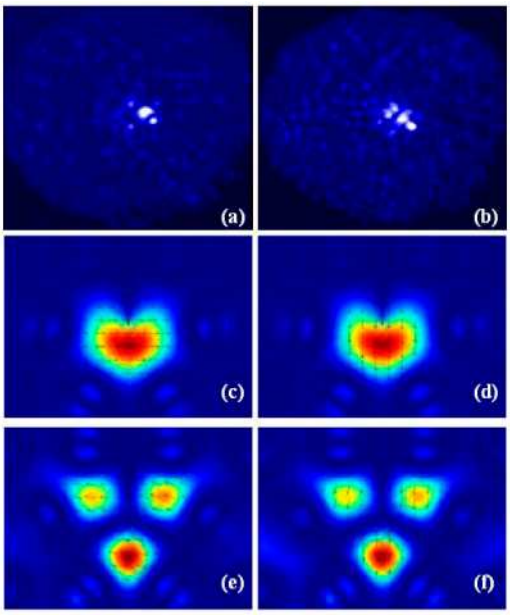

Fig. 4. Mode profile of the near field of the sample in Fig. 2(a) when the external RI is 1.32 (a) Fundamental mode (b) LP_{11} cladding mode (c, d) Simulation of the two fold symmetry LP_{01} core mode (e, f) Simulation of the two fold symmetry LP_{11} like cladding mode.

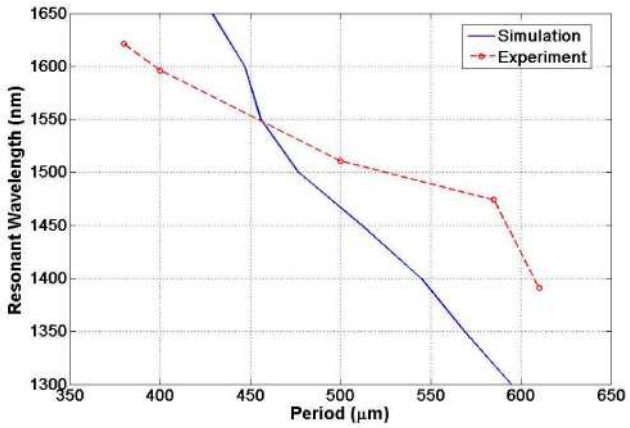

Fig. 5. Phase matching curve for coupling between fundamental mode and LP_{11} like cladding mode (Solid line: simulation result; Broken line: experimental result).

The phase matching curve for the coupling between the fundamental mode and the LP_{11} cladding mode is also simulated by FEM, as shown in Fig. 5. For the purpose of comparison, the experimental phase matching curve (data shown in Fig. 2(b)) is also plotted in Fig. 5. Both the curves show the decrease in resonant wavelength when the grating period increases. The difference between the simulation and the experiment results may be caused by the dimension unconformity among the actual microholes, as a slight deviation of the laser focus spot at the cladding surface leads to a large shift of the microhole tip in the fiber core, which strongly affects the structural modulated RI change.

4. Refractive index sensing

The sample in Fig. 2(a) is also immersed in different RI liquids (Cargille LABS) to measure the resonant wavelength change before being cut off. The sample is first immersed in one RI

#120871 - $15.00 USD Received 2 Dec 2009; revised 11 Jan 2010; accepted 11 Jan 2010; published 19 Jan 2010

liquid and then cleaned by isopropanol until its transmission spectrum matches that in air, before being immersed in another RI liquid. When the external RI changes from 1.30 to 1.35, the resonant wavelength shift is 23.7nm (from 1485.6 to 1509.3nm). The average external RI sensitivity in the range 1.30-1.35 is estimated as 537nm/RIU (through linear interpolation).

According to [17], the detection limit of RI sensing is defined as $DL=R/S$, where R is the sensor resolution and S is the sensitivity. R can be estimated as follows: 1) the amplitude noise (with an assuming SNR of 60dB) $\sigma_{amp}=\Delta\lambda/(4.5SNR^{0.25})$; 2) the temperature stabilization is neglected here; 3) the 0.5nm OSA resolution has a uniform error distribution and thus $\sigma_{spe}=0.5/(12)^{1/2}\approx 0.14$nm. And $\sigma\approx(\sigma_{amp}^2+\sigma_{spe}^2)^{1/2}$ can be used to estimate the error of the resonant wavelength. The DL is estimated to be 4×10^{-3} RIU. The RI sensing results obtained are shown in Fig. 6. The error performance is not very good since the 3-dB bandwidth $\Delta\lambda$ is quite large (~90nm).

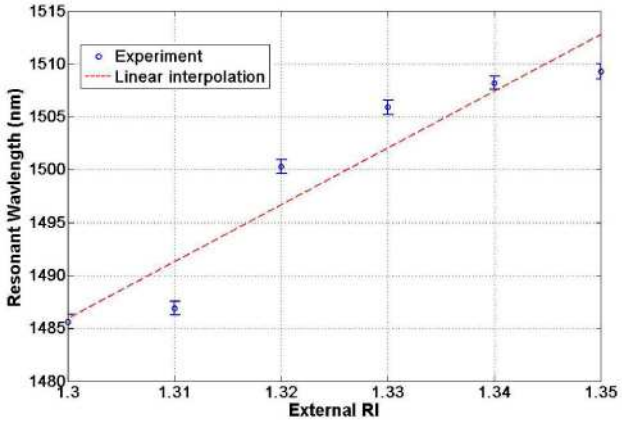

Fig. 6. Resonant wavelength shift of the sample shown in Fig. 2(a) when the external RI changes from 1.30 to 1.35 (Circles: experiment data with error bar; Broken line: linear interpolation).

Compared with LPFGs written in normal SMF of similar periods (~50nm/RIU) [18,20], the relatively high external RI sensitivity of the resonant wavelength change obtained has potential applications in RI sensing in the range far from the fiber cladding (e.g., around water). Since the microhole structure strongly affects the core mode, the external RI change will lead to the effective RI change of the core mode and the cladding mode simultaneously. Thus, the dispersion of both the core mode and the cladding mode needs to be taken into account, while for LPFG in SMF [19], only the cladding mode stands for the RI sensitivity.

The present RI sensitivity is not as high as that reported (~1500nm/RIU) in photonic crystal fiber (PCF) based refractometer [20]. However, the proposed struncure is more convenient for external RI sensing as no infiltrating liquid into the PCF is required, the process of which is difficult and time-consuming [20]. Another advantage of the device proposed over the PCF based refractometer is that the liquid sample can be flexibly changed after each measurement.

5. Conclusion

In conclusion, a new type of LPFG is fabricated by use of femtosecond laser to drill periodical microholes along the longitudinal direction of all-solid PBGF. The variation in waveguide structure results in a strong RI modulation in both the fiber core and the cladding and thus resulting in a compact device dimension. The modes involved in the coupling are analyzed and compared through experiments and simulations. The LPFG developed has potential applications in fiber based external RI sensing within the RI range from 1.30 to 1.35.

#120871 - $15.00 USD Received 2 Dec 2009; revised 11 Jan 2010; accepted 11 Jan 2010; published 19 Jan 2010

Acknowledgement

This work was supported by Hong Kong SAR government through a GRF grant PolyU 5306/08E. The authors would like to thank Yangtze Optical Fiber and Cable (YOFC) Ltd. for providing the PBGF.

#120871 - $15.00 USD Received 2 Dec 2009; revised 11 Jan 2010; accepted 11 Jan 2010; published 19 Jan 2010